THE LANCET
Planetary Health

Supplementary appendix

This appendix formed part of the original submission and has been peer reviewed. We post it as supplied by the authors.

Supplement to: Gelfand MJ, Jackson JC, Pan X, et al. The relationship between cultural tightness–looseness and COVID-19 cases and deaths: a global analysis. *Lancet Planet Health* 2021; published online Jan 29. http://dx.doi.org/10.1016/S2542-5196(20)30301-6.

The Relationship Between Cultural Tightness-Looseness and COVID-19 Cases and Deaths: A Global Analysis
Supplementary Appendix

Table of Contents

Supplemental Methods

Measurement of Cultural Tightness

Our measure of cultural tightness was adapted from Gelfand and colleagues,[1] who gathered cross-cultural data on cultural tightness in 33 nations. The scale has been used to predict a wide range of phenomena, including national differences in creativity rates,[2] CEO discretion,[3] stock price synchrony,[4] leadership preference,[5] expatriate success,[6] global differences in prejudice,[7] and other outcomes.[8] We used the same 6 item scale to assess TL as in our original study (e.g., "In this country, if someone acts in an inappropriate way, others will strongly disapprove") and gathered data on the measure across 57 nations.[9] We note that the TL scores from this new study correlate very highly (r = .87, p < .0001) with the original Gelfand and colleagues[1] scores, suggesting that the scale has good validity. The preregistration of this study is available on OSF at https://osf.io/qg6xy and the scores can be found on page 46 of this Appendix. As in the original study, responses were mean-centered within participants to control for responses sets. The nation-level reliability was .83 and the individual-level reliability was α = .70. A multi-level confirmatory factor analysis (CFA) showed acceptable SRMR (.04), RMSEA (.09), and CFI (.93) indicators.

Evolutionary Game Theoretic Models

In the COVID-19 pandemic, cooperative behaviors among the population such as practicing physical distancing and wearing face masks—which are costly for an individual but have a greater benefit for others—are important for controlling the pandemic. To complement our COVID-19 field data, we developed an evolutionary game theoretic model to examine the effects of tightness-looseness on people's cooperative behaviors under threat. These models do not aim to fully explain our observed data, nor are they designed to specifically model pandemics, but they do offer a potential mechanism for how group-based differences may account for cultural variation in response to an existential threat.

Previous evolutionary game theory models have shown that under conditions of high threat—where payoffs are reduced for a population of agents—mutual cooperation becomes essential for the population's survival.[10] When threat is high and agents are connected in a fixed network,[11] clusters of cooperative agents survive and cooperation spreads across the network. In the current geopolitical context, reduced payoff rates may represent the negative effects of COVID-19 on everyone's well-being, and the demand for cooperation represents a heightened need for behaviors such as physical distancing or wearing face masks.

To date, there have been no computational models that have examined how tight and loose cultures respond to increasing collective threat. We suggest that groups showing high levels of conformity (cultural tightness) should respond faster and more effectively to threats such as COVID-19. When there is no threat, the heightened conformity is not necessarily functional, because cooperative and defective behaviors are similarly effective under low selection pressure from the environment. But in the context of threat, group-based cooperation emerges as essential,[10] and high conformity will allow cooperation to quickly spread across a population of agents.

We illustrate this dynamic for the first time in an evolutionary model of agents playing a Donation Game, which is a special case of the Prisoner's Dilemma (see Table S1).[12] Agents are embedded in a 20 × 20 toroidal (i.e., wrap-around) grid. Each location (x, y) has four neighbor locations: $(x + 1, y)$, $(x - 1, y)$, $(x, y + 1)$, and $(x, y - 1)$. We note below that we also replicated our results with a larger sample in a 50 × 50 grid. Each agent has a strategy, which is either *cooperate* or *defect*. The simulation starts with a grid that is fully occupied by agents whose strategies are chosen randomly, with both strategies being equally likely. Then the simulation repeatedly performs the following sequence of updating steps.

1) *Immigration*: At a randomly chosen empty site, if there is any, a new agent appears whose strategy is equally likely to be *cooperate* or *defect*.

2) *Interaction*: In each iteration, each agent gets a *base payoff* = 30 from the environment, independent of payoffs it gets from interactions. Each agent also plays donation games (Table S1) with all of its alive neighbors, if any, on the grid, and receives *interaction payoffs* from the games. Agents' actions are chosen according to their strategies, which is either cooperate or defect. In the donation games, cooperating means spending a cost of c for the partner in the game to receive a benefit of b. The quantity $k = b / c$, where $k > 1$, represents how much each contribution from a cooperator can be effectively transformed to a larger benefit for others. If both individuals in the game *cooperate* (i.e., each contributes c), then each receives the benefit b, hence each individual's net payoff is $b - c$. If one individual cooperates and the other *defects* (refuses to contribute), then the cooperator contributes the cost and the defector gets the benefit, so their net payoffs are $-c$ and b, respectively. If both individuals defect (i.e., neither contributes), then no benefit is generated, so each gets payoff 0. All the pairs in the grid play the games in a random order.

In addition, agents are subject to a specific level of threat that is implemented as a deduction of τ from everyone's total payoff.[10] Thus, an agent's final payoff, π, in each iteration is as defined in Eq. 1. These payoffs are not cumulative across iterations.

$$\pi = \textit{base payoff} + \textit{interaction payoff} - \tau. \qquad (1)$$

This final payoff is transformed into an agent's fitness, $f(\pi)$, based on the well-established principle of diminishing marginal utility, as shown in Eq. 2 and Figure S1.

$$f(\pi) = \begin{cases} 1 - e^{-0.1 \cdot \pi}, & \text{if } \pi \geq 0; \\ 0 & \text{, if } \pi < 0. \end{cases} \qquad (2)$$

3) *Reproduction*: Each agent is chosen in a random order and given a chance to reproduce with a probability equal to its fitness. Reproduction means creating an offspring in a randomly selected adjacent empty site, if there is any. The offspring is a new agent that usually will have the same strategy as its parent, but there is a small probability $\mu = 0.05$ that it will instead have a randomly selected strategy, chosen in the same way as in Step 1.

4) *Death*: In each iteration, an agent has a probability d to die. The death probability of an agent is a function of its fitness, $f(\pi)$, defined by Eq. 3. As an agent's fitness increases, the death probability of the agent decreases as shown in Figure S2. If an agent dies, it will be removed from the grid.

$$d = e^{-2.3 \cdot f(\pi)} \qquad (3)$$

5) *Conform*: In each iteration, after Step 4, each agent has a probability l of adopting the modal strategy in its neighborhood. If the agent's location is (x, y), the neighborhood locations include (x, y), $(x + 1, y)$, $(x - 1, y)$, $(x, y + 1)$, $(x, y - 1)$, $(x + 1, y + 1)$, $(x + 1, y - 1)$, $(x - 1, y + 1)$, and $(x - 1, y - 1)$. This is a broader range than the neighbors that an agent interacts with because we assume that people can observe more people than they interact with. If there are multiple modal strategies in the neighborhood (i.e., there are equal number of cooperators and defectors), the agent randomly selects one of the multiple modal strategies.

We ran the above updating steps iteratively for 15,000 iterations in each simulation run.

The key parameters of this model intended to represent ecological threat, manipulated by τ, and cultural tightness, manipulated by l. Consistent with past work,[10] we operationalized ecological threat via payoff structure, such that highly threatening environments reduced the maximum payoff that agents received. We implemented a gradually escalating threat which started at a low level ($\tau = 5$) and escalated every 1,500 iterations and reached its maximum value ($\tau = 27.5$) in the 13,500th iteration of the model. Cultural tightness is operationalized by a probability l of conforming with the local norm.

The two outcome variables are cooperation rate, defined by the proportion of alive agents who have a cooperative strategy, and alive rate, defined by the proportion of grid locations that are occupied by agents.

We ran 100 simulation runs representing a loose culture in which agents have a low probability l of conforming to the modal strategy of their neighbors ($l = .05$), whereas another 100 runs represented a tight culture in which agents have a higher probability of conforming ($l = .20$). In the donation game, we set $c = 1$, $b = 3$, and $k = 3$, which is typically the case in research on the evolution of cooperation.[10]

Figure S3 shows that, in the early stages of the model where threat was low, tight and loose cultures both had relatively low cooperation rates. However, as time passed and threat levels escalated, mutual cooperation became more essential and agents in tight cultures adopted cooperative behavior more rapidly than agents in loose cultures. Since mutually cooperative agents received higher joint payoffs than defecting agents, agents in tight cultures had higher survival rates than agents in loose cultures. This suggests that strong normative conformity can be beneficial during periods of intense threat when agents are facing stronger pressure to adopt more effective strategies.

We also ran the models under a variety of other levels of tightness with the same payoff matrix to replicate our effects. Figure S4 shows the results when $l = [0.1, 0.15, 0.3, 0.4, 0.5]$. In the early stages of the model where threat was low, both tight and loose cultures had relatively low cooperation rates and high alive rates. However, as time passed and threat levels escalated, tightness bolstered cooperation and agents in tight cultures were able to have higher alive rates than agents in loose cultures.

Note that in Figures S3 and S4, in the tight cultures, the standard error of the cooperation rates is large, especially under low threat. This is because in some of the single runs, most of the population cooperated under low threat while in some other runs, the majority defected (see Figure S5).

We also tested the robustness of the model by using a narrower range of the conforming neighborhood. Figure S6 shows the results from a model in which each agent conforms only to its four adjacent neighbors (excluding the agent itself). 50 runs were run in a tight culture ($l = .20$) and 50 runs were run in a loose culture ($l = .05$). Under moderate-to-severe levels of threat, a tight culture had a higher cooperation rate and thus a higher alive rate.

Finally, to test the robustness of our results under different sample sizes, we ran 50 simulations in a tight culture ($l = .20$) and 50 simulations in a loose culture ($l = .05$) in a larger network, where agents were embedded in a 50 × 50 wrap-around grid network. The same payoff matrix was used as in the main model. Enlarging the sample size makes no meaningful difference to the results (see Figure S7).

Supplemental Results

Robustness Check Accounting for the Nested Effect of Geographic Regions

A common concern for cross-cultural models involves spatial autocorrelation, or "Galton's problem," which refers to the possibility that data-points are not truly independent. In analyses of pre-industrial societies, for example, it is common to control for language families in order to properly model the shared phylogenetic history of societies. These sorts of controls are less common for nation-level cross-cultural analyses, but they are sometimes important because spatial autocorrelation can violate the assumption that data points are independent. With respect to our data, data points may not have been truly independent because a COVID-19 outbreak in one nation (e.g. Italy) makes it possible that other nations within the same continent (e.g. France, Great Britain) will experience an outbreak. In our model diagnostics, we observed no problematic autocorrelation between model residuals. Nevertheless, we conducted a robustness check to examine whether our findings were influenced by the nestedness of geographic regions to which the countries belong. To do so, we treated geographic region as a cluster variable and standard errors of the model parameter estimates were computed using the sandwich estimator to correct for potential sampling differences across geographic regions (i.e., continents). The sandwich estimator is used for cluster samples in which the clusters are independent but the observations within a cluster are not.[13–15] This model is displayed in Table S2 for COVID-19 cases and Table S3 for COVID-19 deaths. Both models showed a robust effect of cultural tightness.

Additional Control Variables

We replicated our models with several other controls. Research on cross-cultural variation in the spread of COVID-19 has linked this variation to relational mobility (the extent to which it is easy to form new relationships and terminate new ones in a society), such that nations with higher levels of relational mobility had faster growth rates compared to those with lower levels of relational mobility in the first 30 days of COVID-19.[15] Since relational mobility is correlated with tightness across cultures,[16] we sought to test whether our patterns remain the same when controlling for relational mobility. These analyses are summarized in Table S4 for COVID-19 cases and Table S5 for COVID-19 deaths, and they show the same trends as our primary models. The sample size in this analysis is very low given non-overlapping data in the datasets but the effects of tightness are in the predicted direction.

We next examined climatological variables. Past research has linked variation in human culture to temperature and rainfall which could also plausibly predict variation in COVID-19 cases and deaths. To ensure that our effects were not driven by climate, we replicated our results controlling for measures of heat stress, cold stress, and precipitation stress. Results controlling for these variables are summarized in Table S6 for COVID-19 cases, and Table S7 for COVID-19 deaths. We also controlled for mandated Bacillus Calmette-Guérin (BCG) vaccination which has been shown to be related to COVID-19 cases and deaths[17] (Tables S8-S9), logged population size (Tables S10-11), and for the number of SARS cases that each country had (Tables S12-13). In each case, the effect of tightness remains robust.

Interaction of Tightness and Collectivism

We also tested the interaction between tightness and collectivism. Research has reported an interaction between collectivism and a measure of value consensus (i.e., standard deviations of World Value Survey) on cases and deaths during an early 30-day timeframe[18]. However, these analyses were not based on a direct measure of the strictness of social norms and punishments, were focused on a very narrow timeframe, and didn't control for important covariates such as testing, GDP per capita, and inequality. In our data, cultural tightness did not interact with collectivism to predict cases (b = -0.17, SE = .24, t = -0.72, p = .48) or deaths (b = -0.35, SE = .33, t = -1.05, p = .30). These analyses are summarized in Table S14 for COVID-19 cases and Table S15 for COVID-19 deaths.

Interaction of Tightness and Government Efficiency

In early stages of the pandemic (i.e., April 2020), we found that tightness interacted with government efficiency such that tight cultures with efficient governments experienced the fewest cases and deaths. However, this interaction declined over time, while the effects of tightness remained strong and significant. Our analyses illustrate that tightness did not interact with government efficiency to predict cases (b = 0.39, SE = .22, t = 1.76, p = .087) or deaths (b = -0.10, SE = .32, t = -0.31, p = .76) by October of 2020. These analyses are summarized in Table S16 for COVID-19 cases and Table S17 for COVID-19 deaths.

Alternative Underreporting Metrics for Deaths

As noted in the main text, COVID-19 deaths are less likely to be underreported than COVID-19 cases. Many COVID-19 cases are asymptomatic, and people who are asymptomatic are unlikely to be tested, yet people who die from COVID-19 generally express some symptoms. For this reason, underreporting rates is less relevant when analyzing COVID-19 deaths. We note, our results were unchanged regardless of whether or not we controlled for test-case ratio or other measures of underreporting (see Table S18).

Model Diagnostics for COVID-19 Cases

We evaluated the robustness of our models by checking for (a) problematic multicollinearity, (b) heteroscedasticity, and (c) problematic residuals. We estimated multicollinearity via the variance inflation factors for each of our fixed effects. A variance inflation factor of above 5 generally means that a model has high multicollinearity which is biasing the estimates and standard errors. Table S19 shows that no variables had problematic multicollinearity.

We next examined problematic heteroscedasticity. If variation is systematically larger at high or low predicted values in a regression, it can violate OLS model assumptions. To evaluate potential heteroscedasticity, we plotted our model residuals against our model predicted values. There was little systematic invariance in the relationship between residuals and predicted values. For example, the relationship between residuals and predicted values was almost zero, $r < -.001$, $p > .99$, indicating no systematic autocorrelation. This plot (see Figure S8) does suggest that the variance is higher for a few of the lower fitted values. For example, China, Vietnam, Ghana, and India have low predicted values for our analysis of cases. To ensure they weren't affecting our results, we conducted our analysis again excluding India, Ghana, China, and Vietnam, and found the same result: Tightness is associated with cases per million ($b = -.93$, $p < .0001$).

Finally, we examined potentially problematic outliers in our analyses of case rates via studentized residuals. An outlier analysis identified Thailand as the case with the highest studentized residual (-3.21, $p = .0026$). This value was not significantly larger than the average studentized residual when we conducted an outlier test with the appropriate Bonferroni correction ($p = .13$).[19] Moreover, the significant effect of cultural tightness on cases replicated even excluding Thailand ($p = .0002$) from the analysis.

Model Diagnostics for COVID-19 Deaths

We evaluated the robustness of our models for mortality rates by checking for (a) problematic multicollinearity, (b) heteroscedasticity, and (c) problematic residuals**.** We estimated multicollinearity via the variance inflation factors for each of our fixed effects, which included our covariates. As noted above, a variance inflation factor of above 5 generally means that a model has high multicollinearity which is biasing the estimates and standard errors. Table S20 shows that no variables had problematic multicollinearity.

We next examined problematic heteroscedasticity. If variation is systematically larger at high or low predicted values in a regression, it can violate OLS model assumptions. To evaluate potential heteroscedasticity, we plotted our model residuals against our model predicted values. There was little systematic invariance in the relationship between residuals and predicted values. For example, the relationship between residuals and predicted values was almost zero, $r < .001$, $p > .99$, indicating no systematic autocorrelation. This plot (see Figure S9) suggests that the variance is higher for a few of the lower fitted values. For example, Ghana, India, and Sri Lanka have low predicted values for our analysis of deaths. To ensure they weren't affecting our results, we conducted our analysis again excluding Ghana, India, and Sri Lanka, and found that tightness remains robustly associated with deaths per million ($b = -1.25$, $p = .0001$).

We examined potentially problematic outliers in our analyses of mortality via studentized residuals. An outlier analysis identified Vietnam as the case with the highest studentized residual (-2.57, $p = .014$). This value was not significantly larger than the average studentized residual when we conducted an outlier test with the appropriate Bonferroni correction ($p = .75$).[19] Moreover, the significant effect of cultural tightness on deaths replicated when excluding Vietnam ($p = .0003$) from the analysis.

Excluding China and Russia

Because some people are skeptical that China and Russia have been reporting accurate COVID-19 data, we excluded these countries from our analyses with cultural tightness and our main controls. The effect of cultural tightness on cases and deaths was robust to these exclusions. For COVID-19 cases, the effect of cultural tightness also replicated when excluding Russia ($p = .0004$) and China ($p = .0004$) from the analysis (Table S21). For COVID-19 deaths, the significant effect of cultural tightness also replicated when excluding Russia ($p = .0004$) and China ($p = .0003$) (Table S22).

Exploratory results of fear of COVID-19 in tight and loose cultures

Our previous research has shown that collective threat is related to the activation of fear.[20] Yet do tight and loose cultures have different levels of fear during a collective threat? Here we explored this question with data from YouGov, which is a UK-based research and data-analytics group that conducts surveys around the world on a wide variety of topics, including politics, current affairs, and health. Starting February 21, 2020, they began asking people around the world how scared they were that they would contract COVID-19, with potential answers ranging from (1) I am very scared that I will contract the Coronavirus (COVID-19), (2) I am fairly scared that I will contract the Coronavirus (COVID-19), (3) I am not very scared that I will contract the Coronavirus (COVID-19), and (4) I am not at all scared that I will contract the Coronavirus (COVID-19) (with additional options of Don't Know and Not Applicable, I have contracted the Coronavirus). YouGov provides publicly available data on the % of people who said they are "very" or "somewhat" scared that they will contract COVID-19 for representative samples from 25 countries. We were able to analyze 22 countries that had overlapping data with cultural tightness and our controls from February 21st until September 24th. The data can be downloaded from this page and are illustrated in the YouGov Figure below. https://yougov.co.uk/topics/international/articles-reports/2020/03/17/fear-catching-covid-19

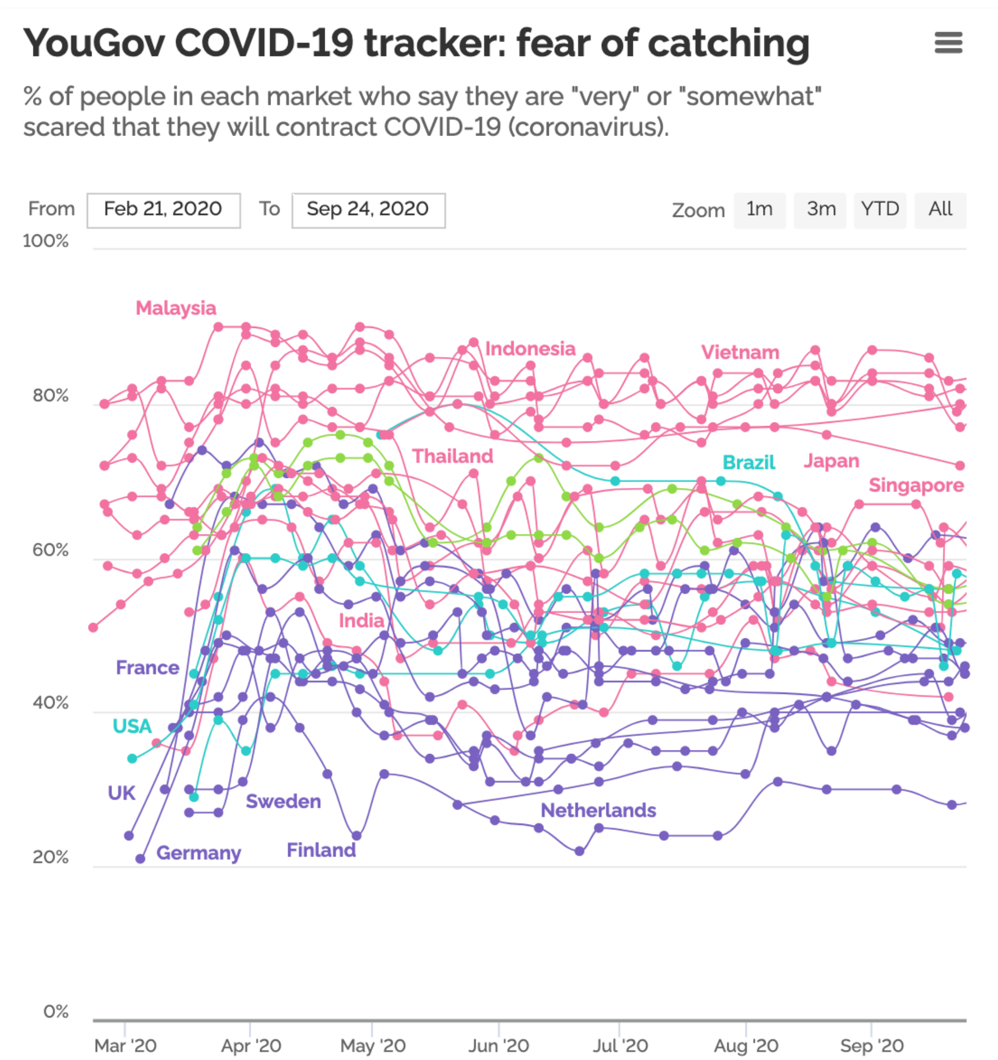

We analyzed two measures of fear response, including the % fear score over the first 100 days after the country had its 1st COVID-19 case and the % fear score for the entire period from February 21st to September 24th. Correlation analysis showed that tightness was positively and significantly correlated with the % of people who were scared of contracting COVID-19 over the first 100 days since the first COVID-19 case, $r = .53$ ($p = .010$), and tightness was positively and significantly related to the % fear score aggregated over the entire period, $r = .49$ ($p = .020$). To put this in context, nations with high levels (z-score = 1) of cultural tightness had a much higher percentage of people who were scared of catching COVID-19 (71% when aggregated over the first 100 days and 70% when aggregated over the entire study period) than nations with high levels (z-score = -1) of cultural looseness (52% when aggregated over the first 100 days and 49% when aggregated over the entire study period).

Fear was negatively and significantly correlated with cases per million on Oct. 16 across countries over the first 100 days, $r = -.47$ ($p = .027$) and over entire study period, $r = -.47$ ($p = .023$). Fear was also negatively and significantly correlated with deaths per million on Oct. 16 across countries over first 100 days, $r = -.55$ ($p = .0083$), and over the entire period, $r = -.57$ ($p = .0048$).

We tested fear of catching COVID-19 as a potential mediator linking country-level tightness to number of cases and deaths of the country on Oct. 16, and included our main controls in the analyses. The regression and mediation findings are summarized in Tables S23-S26. Bootstrap analysis revealed a consistently significant mediation effect for fear of catching COVID-19. Countries that have higher tightness scores were more likely to have higher levels of fear of catching COVID-19 and had lower numbers of cases and deaths on Oct. 16. Though we were limited in the number of countries we could include in our analyses, the analysis suggests that fear differs widely across countries with important associations during COVID-19.

Supplemental Figures

Figure S1.
Fitness as a Function of Final Payoff

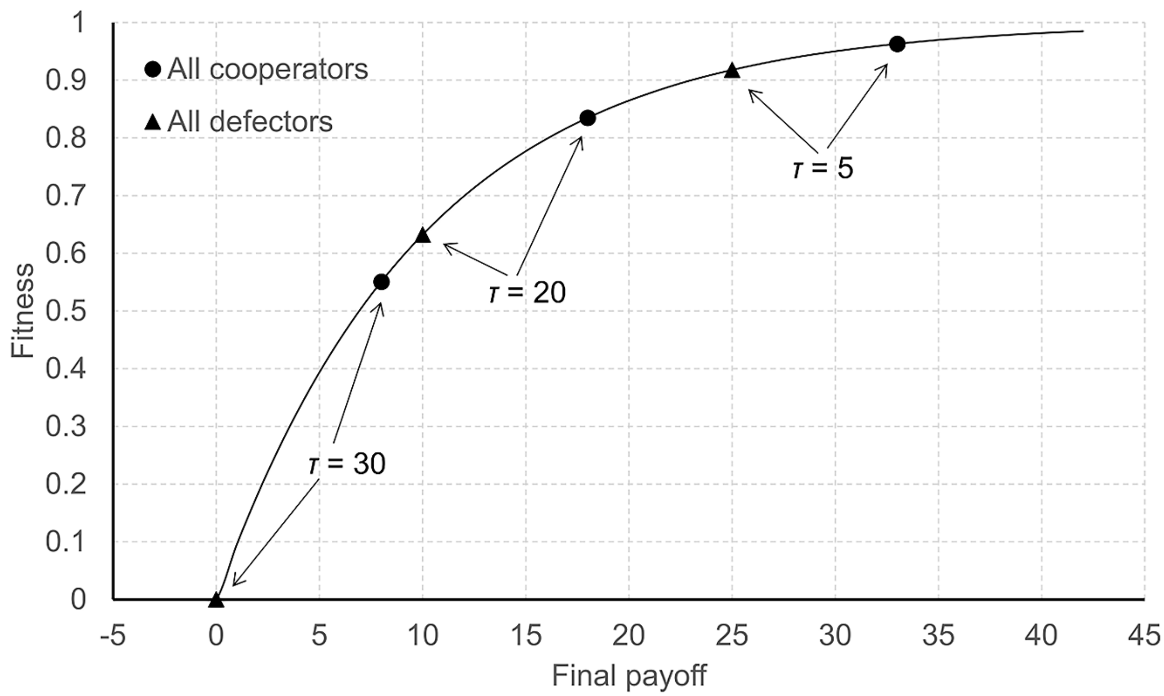

Note. Fitness as a function of final payoff. Circles and triangles, respectively, show the final payoff π and fitness $f(\pi)$ for a cooperator surrounded by cooperators and a defector surrounded by defectors, under three threat levels: high (τ = 30), medium (τ = 20), and low (τ = 5), given b = 3 and c = 1 in the payoff matrix and a base payoff of 30.

Figure S2.
Death Probability as a Function of an Agent's Fitness

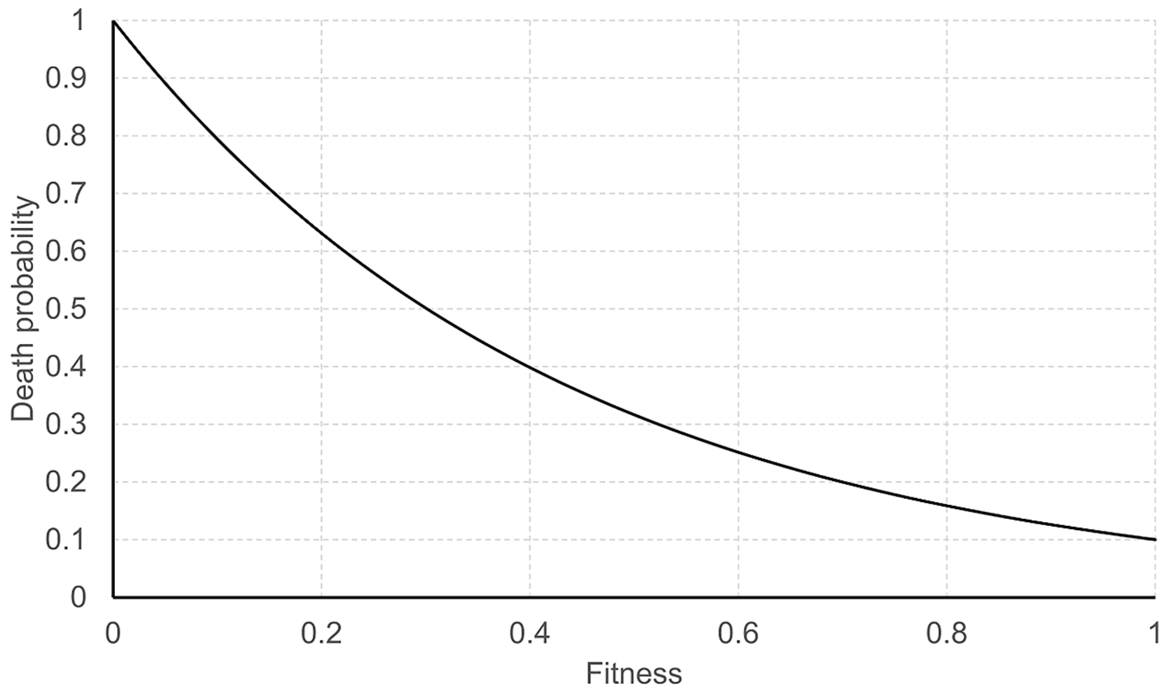

Figure S3.

Cooperation and Alive Rates in a Tight vs. Loose Culture as a Function of Threat

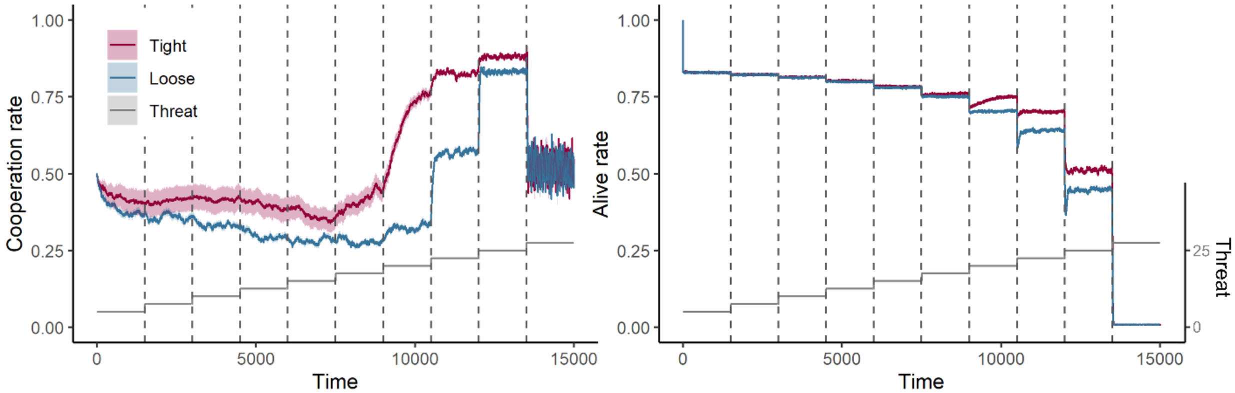

Note. The results of an evolutionary game theoretic model of cooperation in the face of an escalating threat such as COVID-19. The shadow shows standard error. In 100 "tight" runs, agents had a high likelihood (l = .20) of conforming. In 100 "loose" runs, agents had a lower likelihood (l = .05) of conforming to neighbors' decisions. The model also included a level of threat τ which started at a low level (5) and escalated every 1,500 iterations and reached its maximum value (27.5) in the 13,500th iteration. The cost of cooperation c = 1 and the benefit b = 3. The left panel of the plot displays cooperation rates over time, and the right side displays survival rates over time. At the highest level of threat, all agents die out, but at moderate-to-severe levels of threat, tightness bolsters agents' cooperation and survival rates.

Figure S4.

Simulations Under Different Levels of Tightness

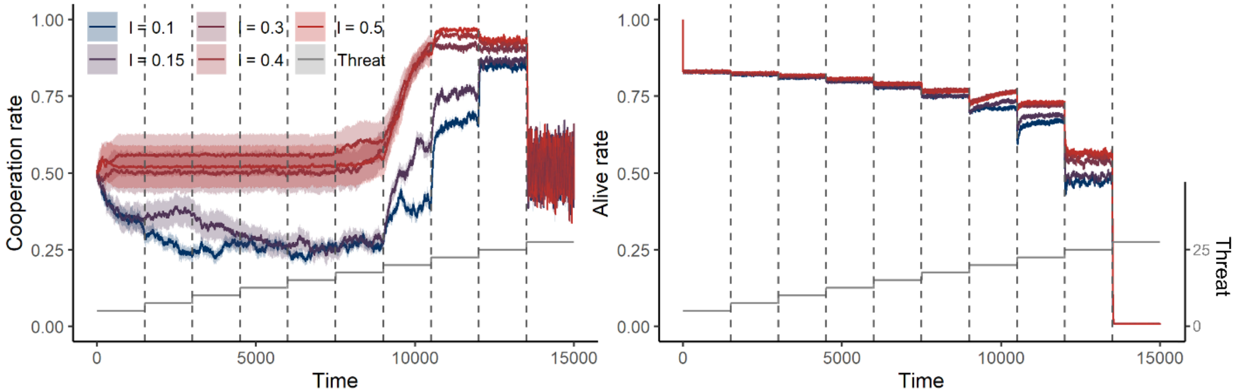

Note. The figure depicts 50 runs at each level of tightness l = [0.1, 0.15, 0.3, 0.4, 0.5], with $b = 3$, $c = 1$, and $k = 3$. Each run contains 15,000 iterations. The shadow shows standard error. The threat τ started at a low level ($\tau = 5$) and escalated every 1,500 iterations, reaching its maximum value ($\tau = 27.5$) in the 13,500th iteration. The left panel shows the results of cooperation rates while the right panel shows the results for alive rates.

Figure S5.

Cooperation Rates in Two Tight Cultures

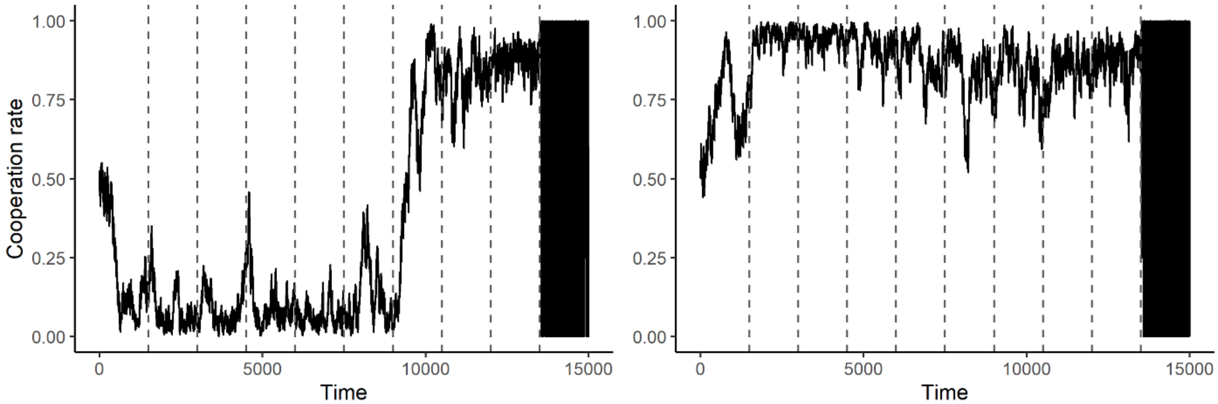

Note. Example of the cooperation rates in two of the tight cultures (l = .20) from Figure S4. On the left, the majority defected when threat was low while on the right, the majority cooperated.

Figure S6.

Simulation Results With a Smaller Neighborhood

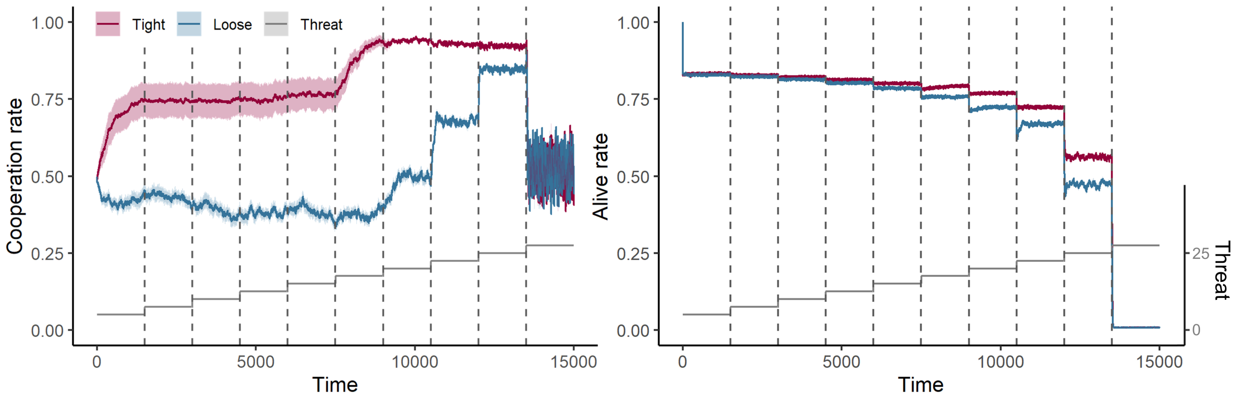

Note. The figure depicts 50 runs in tight (l = .20) and loose (l = .05) cultures where the conforming neighborhood contains only four adjacent neighbors. In this figure, b = 3, c = 1, and k = 3. Each run contains 15,000 iterations. The shadow shows standard error. The threat τ started at a low level (τ = 5) and escalated every 1,500 iterations, reaching its maximum value (τ = 27.5) in the 13,500th iteration. The left panel shows cooperation rates and the right panel shows alive rates.

Figure S7.

Simulation Results With an Expanded Sample Size

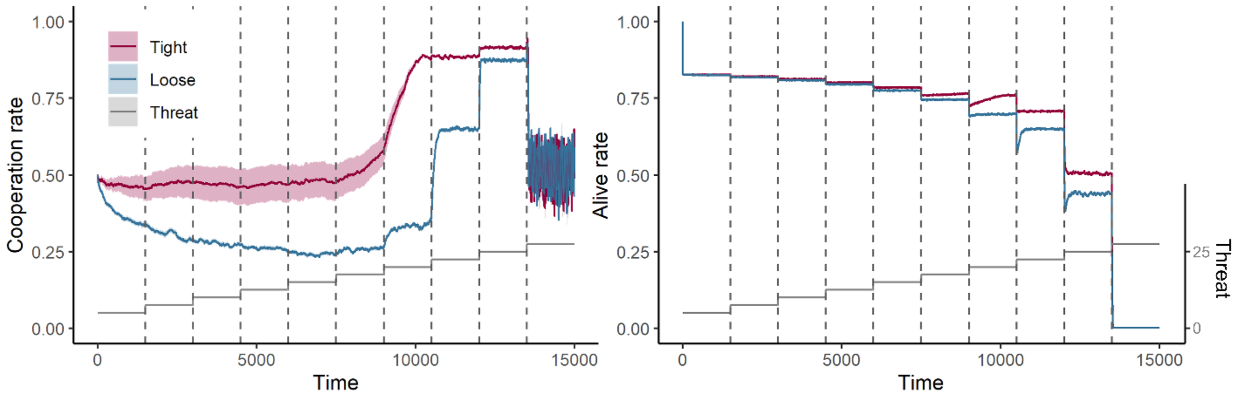

Note. The plots depict the average from 50 runs in a "tight" culture (l = .20) and 50 runs in a "loose" culture (l = .05). Each run has agents embedded in a 50 × 50 wrap-around grid network. The shadows show standard error. The threat τ started at a low level ($\tau = 5$) and escalated every 1,500 iterations, reaching its maximum value ($\tau = 27.5$) in the 13,500th iteration. The left panel shows the results of cooperation rates while the right panel shows the results for alive rates.

Figure S8.

Relationship Between Predicted Values and Model Residuals for Cases per Million

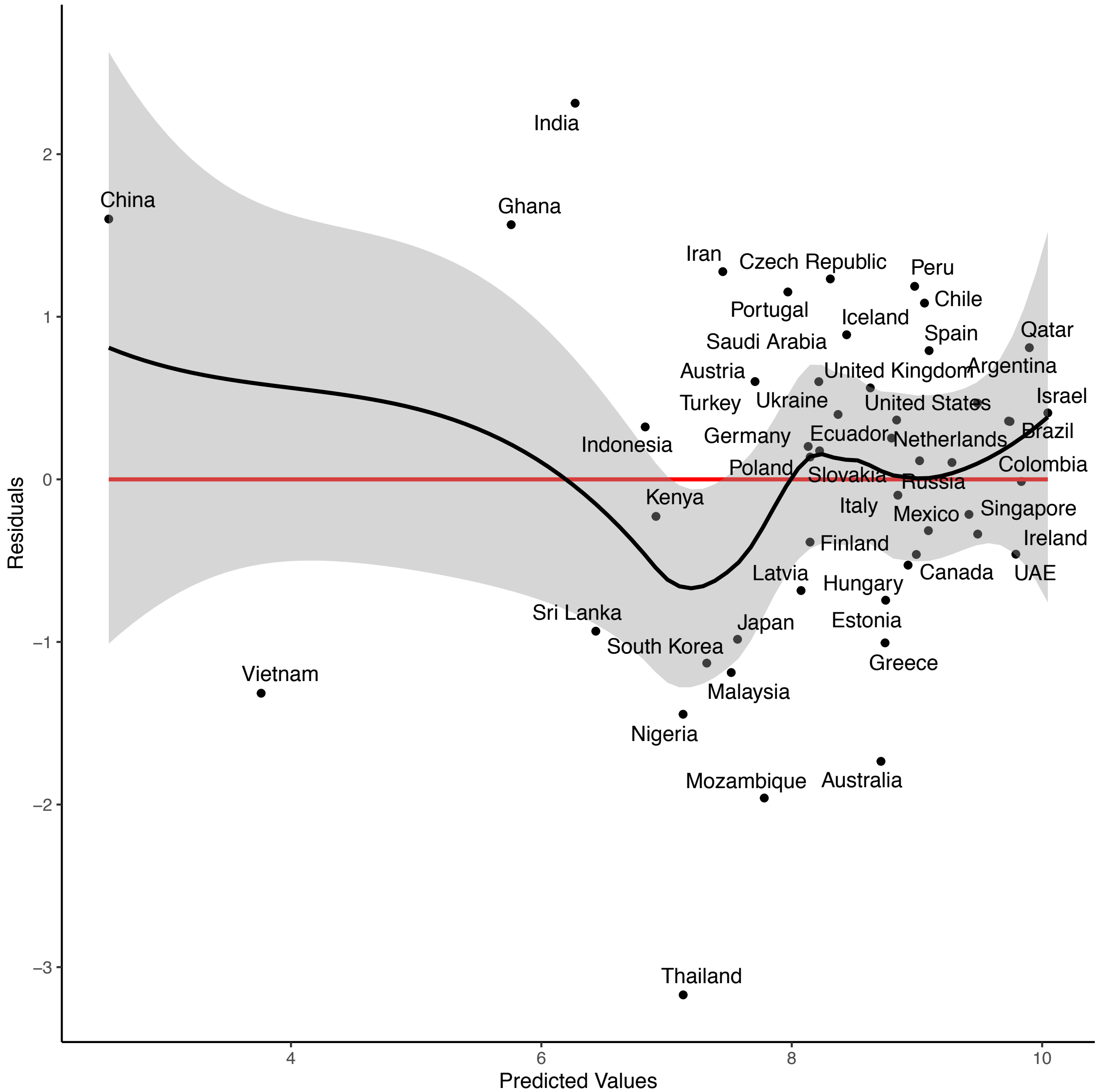

Figure S9.
Relationship Between Predicted Values and Model Residuals for Deaths per Million

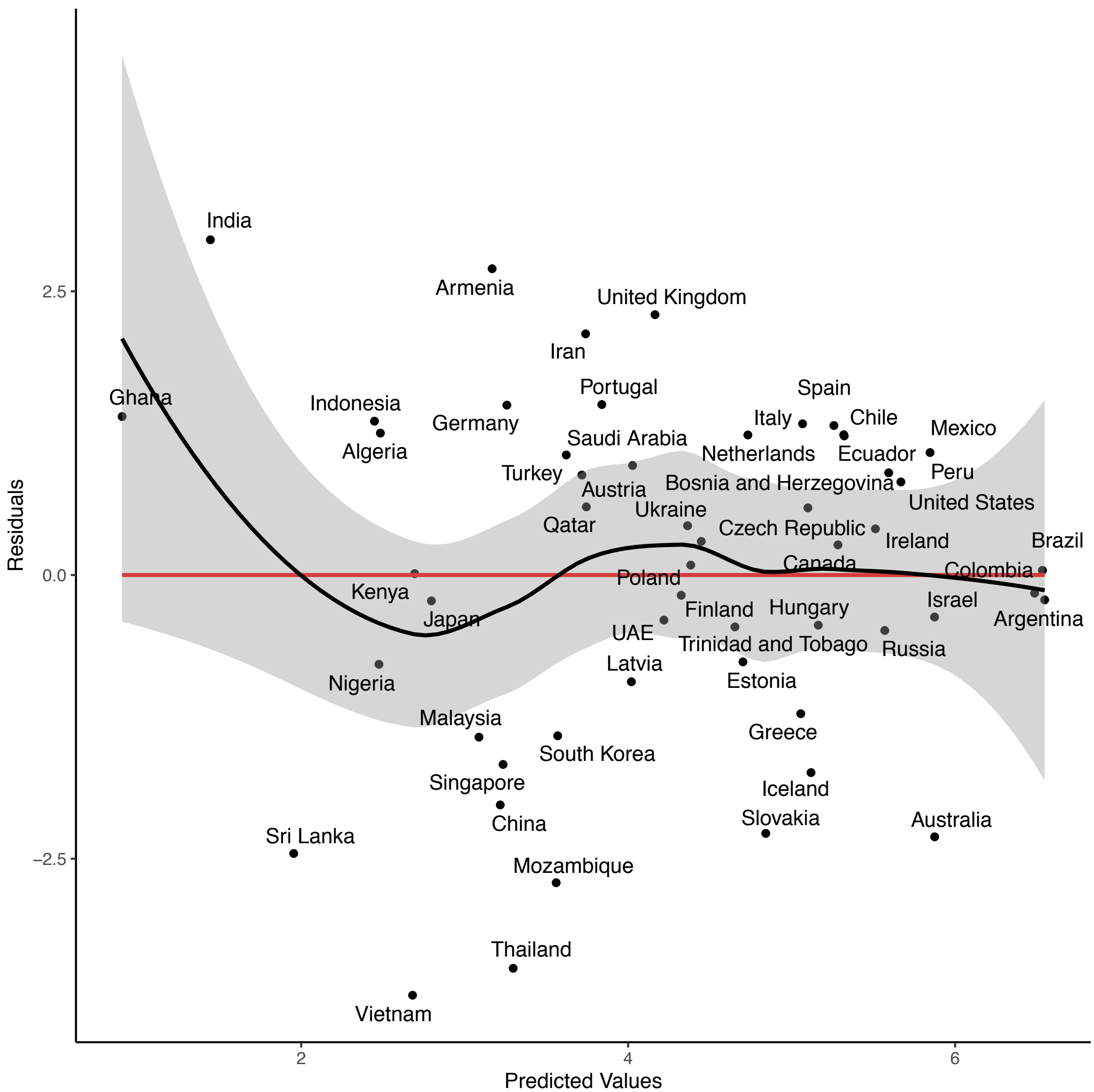

Table S1. Payoff Matrix

Prisoner's Dilemma:

	Cooperate	Defect
Cooperate	(r, r)	(s, t)
Defect	(t, s)	(p, p)

Donation Game:

	Cooperate	Defect
Cooperate	($b-c$, $b-c$)	($-c$, b)
Defect	(b, $-c$)	(0, 0)

Note. A symmetric Prisoner's Dilemma game has the form shown at left, subject to the requirements that $t > r > p > s$ and $2r > t + s$. A Donation Game is a special case of the Prisoner's Dilemma in which r, s, t, and p have the values $b - c$, $-c$, b, and 0, respectively.[12] Here, c is the amount each agent is asked to contribute, and $b = kc$ is the benefit the other agent will get from this contribution, where $k > 1$.

Table S2. Cases Per Million Controlling for Spatial Autocorrelation

	Log of Cases
	Estimate (95% CIs)
Constant	8.11*** (7.85, 8.38)
Test-Case Ratio	-0.82** (-1.29, -.34)
GDP Per Capita	0.44*** (0.25, 0.63)
Gini Coefficient	0.44* (0.04, 0.85)
Population Density	0.00 (-.29, .29)
Percent Migrants	0.59*** (0.45, 0.72)
Gov. Efficiency	-0.19** (-0.34, -0.05)
Tightness	-.81*** (-1.02, -.60)
Observations	50
R^2	0.67
AIC	160.98
BIC	178.19
Sample-size adjusted BIC	149.94
Note:	* p<0.05; ** p<0.01; *** p<0.001

Regions are controlled as sampling clusters and the clustering effect was accounted for by using the sandwich estimator. Predictors standardized

Table S3. Deaths Per Million Controlling for Spatial Autocorrelation

	Log of Deaths
	Estimate (95% CIs)
Constant	4.12*** (3.72, 4.53)
Mortality Rate	-0.34 (-0.92, 0.23)
GDP Per Capita	0.56*** (0.31, 0.81)
Gini Coefficient	0.26 (-0.39, 0.90)
Population Density	-0.27 (-1.05, .52)
Percent Migrants	0.01 (0.00, 0.03)
Gov. Efficiency	-0.67*** (-1.01, -0.32)
Tightness	-1.08*** (-1.21, -0.95)
Observations	55
R^2	0.45
AIC	217.60
BIC	235.66
Sample-size adjusted BIC	207.38
Note:	* p<0.05; **p<0.01 *** p<0.001

Regions are controlled as sampling clusters and the clustering effect was accounted for by using the sandwich estimator. Predictors are standardized.

Table S4. Cases Per Million Controlling for Relational Mobility

	Log of Cases
	Estimate (95% CIs)
Constant	7.78*** (7.37, 8.20)
Test-Case Ratio	-3.84*** (-5.48, -2.19)
GDP Per Capita	0.26 (-0.21, 0.74)
Gini Coefficient	0.37* (0.10, 0.64)
Population Density	-0.06 (-0.35, 0.23)
Percent Migrants	1.13** (0.43, 1.83)
Gov. Efficiency	-0.33 (-0.73, 0.06)
Tightness	-0.46 (-0.95, 0.03)
Relational Mobility	0.24 (-0.09, 0.56)
Observations	22
R^2	0.87
Adjusted R^2	0.79
Residual Std. Error	0.57 (df = 13)
F Statistic	10.98*** (df = 8; 13)
Note:	* p<0.05; ** p<0.01; *** p<0.001

*The number of cases for this analysis was very small because of the low number of available overlapping countries, and thus our statistical power is low. Nevertheless, the effect of tightness is in the predicted direction.

Table S5. Deaths Per Million Controlling for Relational Mobility

	Log of Deaths
	Estimate (95% CIs)
Constant	4.24*** (3.52, 4.95)
Mortality Rate	0.57 (-0.21, 1.34)
GDP Per Capita	0.42 (-0.47, 1.31)
Gini Coefficient	0.59 (-0.11, 1.28)
Population Density	-0.18 (-0.62, 0.26)
Percent Migrants	-0.67 (-1.88, 0.54)
Gov. Efficiency	0.06 (-0.69, 0.81)
Tightness	-0.81 (-1.69, 0.08)
Relational Mobility	0.78* (0.16, 1.41)
Observations	23
R^2	0.72
Adjusted R^2	0.56
Residual Std. Error	1.08 (df = 14)
F Statistic	4.47** (df = 8; 14)
Note:	* p<0.05; ** p<0.01; *** p<0.001

*The number of cases for this analysis was very small because of the low number of available overlapping countries, and thus our statistical power is low. Nevertheless, the effect of tightness is in the predicted direction.

Table S6. Cases Per Million Controlling for Climate

	Log of Cases
	Estimate (95% CIs)
Constant	7.89*** (7.47, 8.30)
Test-Case Ratio	-0.81*** (-1.12, -0.50)
GDP Per Capita	0.46 (-0.06, 0.98)
Gini Coefficient	0.71** (0.27, 1.14)
Population Density	0.12 (-0.24, 0.48)
Percent Migrants	0.66** (0.22, 1.11)
Gov. Efficiency	-0.13 (-0.61, 0.35)
Tightness	-0.66** (-1.12, -0.21)
Cold Stress	0.42 (-0.13, 0.96)
Heat Stress	-0.30 (-0.76, 0.15)
Rain Stress	0.34 (-0.07, 0.74)
Observations	50
R^2	0.73
Adjusted R^2	0.66
Residual Std. Error	1.04 (df = 39)
F Statistic	10.38*** (df = 10; 39)
Note:	* p<0.05; ** p<0.01; *** p<0.001

Table S7. Deaths Per Million Controlling for Climate

	Log of Deaths
	Estimate (95% CIs)
Constant	3.90*** (3.30, 4.50)
Mortality Rate	-0.28 (-0.89, 0.33)
GDP Per Capita	0.46 (-0.31, 1.24)
Gini Coefficient	0.56 (-0.04, 1.15)
Population Density	-0.09 (-0.59, 0.42)
Percent Migrants	0.50 (-0.14, 1.14)
Gov. Efficiency	-0.59 (-1.30, 0.11)
Tightness	-0.81* (-1.45, -0.18)
Cold Stress	0.36 (-0.40, 1.12)
Heat Stress	-0.55 (-1.19, 0.08)
Rain Stress	0.25 (-0.37, 0.87)
Observations	55
R^2	0.52
Adjusted R^2	0.41
Residual Std. Error	1.55 (df = 44)
F Statistic	4.71*** (df = 10; 44)
Note:	* p<0.05; ** p<0.01; *** p<0.001

Table S8. Cases Per Million Controlling for Bacillus Calmette-Guérin (BCG) vaccination

	Log of Cases
	Estimate (95% CIs)
Constant	8.14*** (6.89, 9.39)
Test-Case Ratio	-0.79*** (-1.12, -0.47)
GDP Per Capita	0.31 (-0.31, 0.94)
Gini Coefficient	0.47* (0.09, 0.85)
Population Density	0.07 (-0.31, 0.46)
Percent Migrants	0.63** (0.21, 1.05)
Gov. Efficiency	-0.16 (-0.67, 0.34)
Tightness	-0.86*** (-1.29, -0.43)
Vaccine Current	-0.14 (-1.50, 1.22)
Vaccine Past	0.06 (-1.40, 1.52)
Observations	49
R^2	0.67
Adjusted R^2	0.60
Residual Std. Error	1.13 (df = 39)
F Statistic	8.97*** (df = 9; 39)
Note:	* p<0.05; ** p<0.01; *** p<0.001

Table S9. Deaths Per Million Controlling for Bacillus Calmette-Guérin (BCG) vaccination

	Log of Deaths
	Estimate (95% CIs)
Constant	5.21*** (3.42, 6.99)
Mortality Rate	-0.38 (-0.95, 0.20)
GDP Per Capita	0.40 (-0.48, 1.28)
Gini Coefficient	0.17 (-0.39, 0.72)
Population Density	-0.34 (-0.83, 0.15)
Percent Migrants	0.24 (-0.37, 0.86)
Gov. Efficiency	-0.51 (-1.22, 0.20)
Tightness	-1.03*** (-1.60, -0.47)
Vaccine Current	-1.18 (-3.11, 0.75)
Vaccine Past	-0.61 (-2.70, 1.48)
Observations	53
R^2	0.49
Adjusted R^2	0.38
Residual Std. Error	1.62 (df = 43)
F Statistic	4.52*** (df = 9; 43)
Note:	* p<0.05; ** p<0.01; *** p<0.001

Table S10. Cases Per Million Controlling for Total Population

	Log of Cases
	Estimate (95% CIs)
Constant	8.04*** (7.73, 8.36)
Test-Case Ratio	-0.85*** (-1.18, -0.51)
GDP Per Capita	0.47 (-0.03, 0.96)
Gini Coefficient	0.38 (-0.004, 0.77)
Population Density	-0.03 (-0.37, 0.31)
Percent Migrants	0.63** (0.23, 1.04)
Gov. Efficiency	-0.19 (-0.67, 0.29)
Tightness	-0.82*** (-1.23, -0.42)
Total Population	0.20 (-0.20, 0.61)
Observations	50
R^2	0.68
Adjusted R^2	0.61
Residual Std. Error	1.11 (df = 41)
F Statistic	10.73*** (df = 8; 41)
Note:	* p<0.05; ** p<0.01; *** p<0.001

Table S11. Deaths Per Million Controlling for Total Population

	Log of Deaths
	Estimate (95% CIs)
Constant	4.14*** (3.71, 4.56)
Mortality Rate	-0.28 (-0.84, 0.28)
GDP Per Capita	0.58 (-0.12, 1.29)
Gini Coefficient	0.21 (-0.32, 0.75)
Population Density	-0.33 (-0.78, 0.12)
Percent Migrants	0.36 (-0.24, 0.96)
Gov. Efficiency	-0.58 (-1.26, 0.10)
Tightness	-1.09*** (-1.64, -0.54)
Total Population	0.30 (-0.17, 0.77)
Observations	55
R^2	0.47
Adjusted R^2	0.37
Residual Std. Error	1.60 (df = 46)
F Statistic	5.02*** (df = 8; 46)
Note:	* p<0.05; ** p<0.01; *** p<0.001

Table S12. Cases Per Million Controlling for Number of SARs Cases

	Log of Cases	
	Estimate (95% CIs)	
Constant	8.07 ***	(7.75, 8.39)
Test-Case Ratio	-0.81 ***	(-1.13, -0.49)
GDP Per Capita	0.48	(-0.04, 0.99)
Gini Coefficient	0.40 *	(0.01, 0.78)
Population Density	0.02	(-0.33, 0.36)
Percent Migrants	0.61 **	(0.21, 1.02)
Gov. Efficiency	-0.28	(-0.78, 0.23)
Tightness	-0.75 **	(-1.18, -0.33)
SARS	0.20	(-0.12, 0.51)
Observations	50	
R^2	0.68	
Adjusted R^2	0.62	
Residual Std. Error	1.20 (df = 41)	
F Statistic	11.01** (df = 8, 41)	

Note. * p<0.05; ** p<0.01; ***p<0.001. All predictors were standardized.

Table S13. Deaths Per Million Controlling for Number of SARs cases

	Log of Deaths	
	Estimate (95% CIs)	
Constant	4.13 ***	(3.70, 4.57)
Mortality Rate (2017)	-0.31	(-0.89, 0.26)
GDP Per Capita	0.60	(-0.14, 1.34)
GINI	0.23	(-0.32, 0.78)
Population Density	-0.25	(-0.71, 0.21)
Percent Migrants	0.27	(-0.34, 0.88)
Gov. Efficiency	-0.66	(-1.38, 0.06)
Tightness	-1.01 **	(-1.59, -0.43)
SARS	0.21	(-0.26, 0.67)
Observations	55	
R^2	0.46	
Adjusted R^2	0.36	
Residual Std. Error	2.59 (df = 46)	
F Statistic	4.82** (df = 8, 46)	

Note. * p<0.05; ** p<0.01; *** p<0.001. All predictors were standardized.

Table S14. Interaction Between Tightness and Collectivism on Cases Per Million

	Log of Cases
	Estimate (95% CIs)
Constant	8.16*** (7.78, 8.54)
Test-Case Ratio	-0.81*** (-1.13, -0.48)
GDP Per Capita	0.37 (-0.24, 0.98)
Gini Coefficient	0.43* (0.03, 0.83)
Population Density	0.01 (-0.35, 0.37)
Percent Migrants	0.60** (0.17, 1.02)
Government Efficiency	-0.14 (-0.64, 0.36)
Collectivism	-0.06 (-0.60, 0.47)
Tightness	-0.75** (-1.20, -0.29)
Tightness * Collectivism	-0.17 (-0.64, 0.30)
Observations	49
R^2	0.68
Adjusted R^2	0.60
Residual Std. Error	1.13 (df = 39)
F Statistic	9.00*** (df = 9; 39)
Note:	* p<0.05; ** p<0.01; *** p<0.001

Table S15. Interaction Between Tightness and Collectivism on Deaths Per Million

	Log of Deaths
	Estimate (95% CIs)
Constant	4.23*** (3.71, 4.75)
Mortality	-0.36 (-1.00, 0.27)
GDP Per Capita	0.15 (-0.71, 1.01)
Gini Coefficient	0.56 (-0.05, 1.17)
Population Density	-0.11 (-0.61, 0.39)
Percent Migrants	0.39 (-0.20, 0.99)
Government Efficiency	-0.40 (-1.10, 0.30)
Collectivism	-0.75 (-1.52, 0.03)
Tightness	-0.96** (-1.59, -0.32)
Tightness * Collectivism	-0.35 (-1.00, 0.30)
Observations	50
R^2	0.51
Adjusted R^2	0.40
Residual Std. Error	1.57 (df = 40)
F Statistic	4.70*** (df = 9; 40)
Note:	* p<0.05; ** p<0.01; *** p<0.001

Table S16. Interaction Between Tightness and Government Efficiency on Cases Per Million

	Log of Cases
	Estimate (95% CIs)
Constant	7.95*** (7.62, 8.28)
Test-Case Ratio	-0.79*** (-1.10, -0.48)
GDP Per Capita	0.51* (0.02, 1.00)
Gini Coefficient	0.38 (0.01, 0.74)
Population Density	-0.07 (-0.40, 0.27)
Percent Migrants	0.28 (-0.23, 0.79)
Gov. Efficiency	-0.04 (-0.54, 0.46)
Tightness	-0.76*** (-1.15, -0.36)
Tightness * Gov. Efficiency	0.39 (-0.05, 0.83)
Observations	50
R^2	0.69
Adjusted R^2	0.63
Residual Std. Error	1.08 (df = 41)
F Statistic	11.53*** (df = 8; 41)
Note:	* p<0.05; ** p<0.01; *** p<0.001

Table S17. Interaction Between Tightness and Government Efficiency on Deaths Per Million

	Log of Deaths
	Estimate (95% CIs)
Constant	4.16*** (3.69, 4.64)
Mortality	-0.31 (-0.88, 0.25)
GDP Per Capita	0.53 (-0.20, 1.25)
Gini Coefficient	0.28 (-0.28, 0.83)
Population Density	-0.26 (-0.72, 0.19)
Percent Migrants	0.35 (-0.42, 1.11)
Gov. Efficiency	-0.62 (-1.36, 0.12)
Tightness	-1.09*** (-1.65, -0.52)
Tightness * Gov. Efficiency	-0.10 (-0.73, 0.53)
Observations	55
R^2	0.45
Adjusted R^2	0.35
Residual Std. Error	1.62 (df = 46)
F Statistic	4.69*** (df = 8; 46)
Note:	* p<0.05; ** p<0.01; *** p<0.001

Table S18. Deaths Per Million Controlling for Underreporting Metrics (Oct. 16)

	Log of Deaths				
	Estimate (95% CIs)				
	(1)	(2)	(3)	(4)	(5)
Constant	4.13*** (3.71, 4.56)	4.06*** (3.64, 4.47)	4.04*** (3.58, 4.50)	4.12*** (3.67, 4.57)	4.13*** (3.71, 4.56)
Mortality	-0.31 (-0.87, 0.25)	-0.37 (-0.93, 0.19)	-0.23 (-0.84, 0.37)	-0.20 (-0.80, 0.41)	-0.26 (-0.82, 0.31)
Test-Case Ratio		-0.64** (-1.07, -0.21)			
Tests Per Thousand			-0.02 (-0.83, 0.78)		
DA-CFR Underreporting				0.33 (-0.26, 0.93)	
Hospital Beds Per Thousand					-0.36 (-0.95, 0.23)
GDP Per Capita	0.54 (-0.17, 1.25)	0.52 (-0.15, 1.19)	0.66 (-0.08, 1.40)	0.53 (-0.19, 1.26)	0.64 (-0.08, 1.37)
GINI	0.26 (-0.28, 0.79)	0.33 (-0.25, 0.91)	0.48 (-0.15, 1.11)	0.24 (-0.33, 0.82)	0.12 (-0.45, 0.70)
Population Density	-0.28 (-0.72, 0.17)	-0.23 (-0.68, 0.23)	-0.25 (-0.75, 0.25)	-0.25 (-0.75, 0.26)	-0.27 (-0.71, 0.18)
Percent Migrants	0.27 (-0.32, 0.86)	0.15 (-0.41, 0.71)	0.28 (-0.52, 1.09)	0.21 (-0.40, 0.82)	0.24 (-0.34, 0.83)
Gov. Efficiency	-0.58 (-1.26, 0.10)	-0.42 (-1.06, 0.22)	-0.51 (-1.22, 0.20)	-0.38 (-1.14, 0.38)	-0.63 (-1.31, 0.05)
Tightness	-1.07*** (-1.62, -0.52)	-1.11*** (-1.66, -0.56)	-1.15*** (-1.77, -0.53)	-0.94** (-1.55, -0.34)	-1.15*** (-1.72, -0.59)
Observations	55	50	50	52	55
R^2	0.45	0.57	0.48	0.45	0.46
Adjusted R^2	0.37	0.49	0.38	0.35	0.37
Residual Std. Error	1.60 (df = 47)	1.48 (df = 41)	1.63 (df = 41)	1.64 (df = 43)	1.60 (df = 46)
F Statistic	5.45*** (df = 7; 47)	6.81*** (df = 8; 41)	4.74*** (df = 8; 41)	4.38*** (df = 8; 43)	4.99*** (df = 8; 46)
Note:					* p<0.05; ** p<0.01; *** p<0.001

Table S19. COVID-19 Cases Multicollinearity Analysis

Fixed Effect	**Model *VIF***
Test-Case Ratio	1.06
GDP Per Capita	2.68
Gini Coefficient	1.31
Population Density	1.14
Percent Migrants	1.81
Government Efficiency	2.47
Cultural Tightness	1.67

Table S20. COVID-19 Deaths Multicollinearity Analysis

Fixed Effect	**Model *VIF***
All-Cause Mortality	1.78
GDP Per Capita	2.75
Gini Coefficient	1.54
Population Density	1.06
Percent Migrants	1.94
Government Efficiency	2.53
Cultural Tightness	1.70

Table S21. Cases Per Million Controlling for China and Russia

	Log of Cases	
	Estimate (95% CIs)	
	(1: China)	**(2: Russia)**
Constant	7.97*** (7.68, 8.27)	8.06*** (7.75, 8.38)
Test-Case Ratio	-1.43*** (-1.95, -0.91)	-0.79*** (-1.11, -0.48)
GDP Per Capita	0.44 (-0.02, 0.90)	0.45 (-0.06, 0.95)
Gini Coefficient	0.36* (0.02, 0.71)	0.44* (0.07, 0.81)
Population Density	-0.01 (-0.32, 0.30)	0.001 (-0.35, 0.35)
Percent Migrants	0.60** (0.24, 0.97)	0.58** (0.18, 0.98)
Gov. Efficiency	-0.24 (-0.68, 0.20)	-0.20 (-0.68, 0.28)
Tightness	-0.74*** (-1.11, -0.36)	-0.80*** (-1.21, -0.39)
Observations	49	49
R^2	0.69	0.67
Adjusted R^2	0.64	0.61
Residual Std. Error	1.02 (df = 41)	1.12 (df = 41)
F Statistic	13.16*** (df = 7; 41)	11.75*** (df = 7; 41)
Note:		* p<0.05; ** p<0.01; *** p<0.001

Table S22. Deaths Per Million Controlling for China and Russia

	Log of Deaths	
	Estimate (95% CIs)	
	(1: China)	**(2: Russia)**
Constant	4.17*** (3.74, 4.60)	4.14*** (3.71, 4.58)
Test-Case Ratio	-0.34 (-0.90, 0.22)	-0.30 (-0.88, 0.28)
GDP Per Capita	0.50 (-0.21, 1.21)	0.54 (-0.19, 1.26)
Gini Coefficient	0.25 (-0.29, 0.78)	0.26 (-0.28, 0.81)
Population Density	-0.26 (-0.70, 0.18)	-0.29 (-0.75, 0.17)
Percent Migrants	0.23 (-0.36, 0.82)	0.28 (-0.32, 0.88)
Gov. Efficiency	-0.52 (-1.20, 0.16)	-0.57 (-1.26, 0.11)
Tightness	-1.09*** (-1.64, -0.54)	-1.08*** (-1.64, -0.52)
Observations	54	54
R^2	0.44	0.45
Adjusted R^2	0.36	0.36
Residual Std. Error	1.59 (df = 46)	1.62 (df = 46)
F Statistic	5.25*** (df = 7; 46)	5.30*** (df = 7; 46)
Note:		* p<0.05; ** p<0.01; *** p<0.001

Table S23. Tightness, Fear, and Cases Per Million (Oct. 16) over the first 100 days after the 1st case

	Fear of Catching		**Log of Cases**	
	Estimate (95% CIs)		Estimate (95% CIs)	
Constant	61.23 ***	(56.41, 66.05)	10.64 ***	(8.50, 12.77)
Test-Case Ratio			-1.17 ***	(-1.68, -0.66)
GDP Per Capita	-4.77	(-12.71, 3.18)	0.17	(-0.46, 0.80)
Gini Coefficient	5.07	(-1.06, 11.20)	0.87 **	(0.33, 1.41)
Population Density	-0.07	(-4.47, 4.33)	0.10	(-0.24, 0.44)
Percent Migrants	0.67	(-4.84, 6.17)	0.55 *	(0.13, 0.98)
Gov. Efficiency	-1.76	(-8.09, 4.58)	-0.20	(-0.69, 0.30)
Tightness	9.66 *	(1.66, 17.67)	-0.41	(-1.11, 0.28)
Fear of Catching (100 days from 1st case)			-0.04 *	(-0.08, -0.01)
Indirect Effect (Tightness → Fear of Catching → Log of Cases)	-.40* (-0.97, -0.02)			
R^2	0.55		0.79	
Observations	21			
AIC	250.94			
BIC	269.74			
SS BIC	214.17			

Note. * p<0.05; ** p<0.01; *** p<0.001. The confidence interval of the indirect effect was derived from 20,000 bootstrap samples. South Korea did not have survey data on fear of catching COVID-19 during the first 100 days with cases and thus was not included in this analysis.

Table S24. Tightness, Fear, and Cases Per Million (Oct. 16) over the entire study period

	Fear of Catching		Log of Cases	
	Estimate (95% CIs)		Estimate (95% CIs)	
Constant	59.44 ***	(54.98, 63.91)	10.51 ***	(8.41, 12.6)
Test-Case Ratio			-1.19 ***	(-1.69, -0.70)
GDP Per Capita	-2.89	(-10.32, 4.54)	0.20	(-0.42, 0.81)
Gini Coefficient	4.52	(-1.11, 10.14)	0.90 ***	(0.39, 1.40)
Population Density	1.21	(-2.92, 5.33)	0.13	(-0.21, 0.47)
Percent Migrants	-0.71	(-5.90, 4.48)	0.52 *	(0.10, 0.94)
Gov. Efficiency	-1.66	(-7.38, 4.06)	-0.13	(-0.59, 0.34)
Tightness	10.27 **	(2.79, 17.75)	-0.43	(-1.13, 0.27)
Fear of Catching (Entire Period)			-0.04 *	(-0.08, -0.01)
Indirect Effect (Tightness → Fear of Catching → Log of Cases)	-.42* (-0.99, -0.03)			
R^2	0.54		0.79	
Observations	22			
AIC	258.81			
BIC	278.45			
SS BIC	222.81			

Note. * p<0.05; ** p<0.01; *** p<0.001. The confidence interval of the indirect effect was derived from 20,000 bootstrap samples.

Table S25. Tightness, Fear, and Deaths Per Million (Oct. 16) over the first 100 days after the 1st case

	Fear of Catching		Log of Deaths	
	Estimate (95% CIs)		Estimate (95% CIs)	
Constant	61.23 ***	(56.41, 66.05)	8.98 ***	(6.10, 11.85)
Mortality Rate (2017)			2.54 **	(0.76, 4.32)
GDP Per Capita	-4.77	(-12.71, 3.18)	-1.39 *	(-2.73, -0.05)
Gini Coefficient	5.07	(-1.06, 11.20)	1.87 ***	(0.87, 2.86)
Population Density	-0.07	(-4.47, 4.33)	-0.39	(-0.88, 0.10)
Percent Migrants	0.67	(-4.84, 6.17)	1.75 **	(0.61, 2.88)
Gov. Efficiency	-1.76	(-8.09, 4.58)	0.13	(-0.72, 0.99)
Tightness	9.66 *	(1.66, 17.67)	-0.83	(-1.80, 0.15)
Fear of Catching (100 days from 1st case)			-0.08 **	(-0.12, -0.03)
Indirect Effect (Tightness → Fear of Catching → Log of Deaths)	-0.73* (-1.62, -0.10)			
R^2	0.55		0.71	
Observations	21			
AIC	265.08			
BIC	283.88			
SS BIC	228.31			

Note. * p<0.05; ** p<0.01; *** p<0.001. The confidence interval of the indirect effect was derived from 20,000 bootstrap samples. South Korea did not have survey data on fear of catching COVID-19 during the first 100 days with cases and thus was not included in this analysis.

Table S26. Tightness, Fear, and Deaths Per Million (Oct. 16) over the entire study period.

	Fear of Catching		Log of Deaths	
	Estimate (95% CIs)		Estimate (95% CIs)	
Constant	59.44 ***	(54.98, 63.91)	7.75 ***	(4.33, 11.17)
Mortality Rate (2017)			1.05	(-0.34, 2.44)
GDP Per Capita	-2.89	(-10.32, 4.54)	-0.32	(-1.46, 0.83)
Gini Coefficient	4.52	(-1.11, 10.14)	1.11 **	(0.28, 1.95)
Population Density	1.21	(-2.92, 5.33)	-0.21	(-0.75, 0.33)
Percent Migrants	-0.71	(-5.90, 4.48)	0.83	(-0.15, 1.80)
Gov. Efficiency	-1.66	(-7.38, 4.06)	-0.31	(-1.09, 0.48)
Tightness	10.27 **	(2.79, 17.75)	-0.83	(-1.96, 0.29)
Fear of Catching (Entire period)			-0.06 *	(-0.12, 0.00)
Indirect Effect (Tightness → Fear of Catching → Log of Deaths)	-0.61* (-1.49, -0.01)			
R^2	0.54		0.61	
Observations	22			
AIC	279.34			
BIC	298.97			
SS BIC	243.34			

Note. * p<0.05; ** p<0.01; *** p<0.001. The confidence interval of the indirect effect was derived from 20,000 bootstrap samples.

Appendix S1. Data sources.

Variable	Source(s)	Link
Total Cases Per Million (Oct 16)	OWID. Data downloaded Oct 16, 2020 from https://ourworldindata.org/coronavirus-data For Spain and Sweden, Oct 15th data was used, as Oct 16th data was not yet available.	https://osf.io/47pe8/
Total Deaths Per Million (Oct 16)		
Test-Case Ratio	OWID. Data downloaded on October 16, 2020 from https://ourworldindata.org/coronavirus-data Calculated as Total Tests (Oct 16) / Total Cases (Oct 16), or the closest testing data to this date that was available	https://osf.io/47pe8/
Tests Per Thousand	OWID. Data downloaded on October 16, 2020 from https://ourworldindata.org/coronavirus-data Total Test Per Thousand (Oct 16), or closest testing data to this date that was available	https://osf.io/47pe8/
DA-CFR Underreporting	Russell et al. (Symptomatic Cases Reported, 08-11-2020, downloaded October 22, 2020) The median percentage of symptomatic cases reported in the "Current Estimates of Under-Reporting" tab was transformed by subtracting this value from 1 to get a score of proportion of symptomatic cases that were not reported.	https://cmmid.github.io/topics/covid19/global_cfr_estimates.html
Hospital Beds Per Thousand	OWID (2004 to 2018)	https://ourworldindata.org/grapher/hospital-beds-per-1000-people
GDP Per Capita	World Bank (2019)	https://data.worldbank.org/indicator/NY.GDP.PCAP.CD
Gini Coefficient	*Sources:*	
	World Bank (most countries, most recent data available) Downloaded September 13, 2020	https://data.worldbank.org/indicator/SI.POV.GINI
	Knoema (Slovakia, 2018)	https://knoema.com/atlas/Slovakia/GINI-index
	Knoema (South Korea, 2018)	https://knoema.com/search?query=gini+index+south+korea
	Singapore Government (2019) (Data converted from Gini as ratio to percent to match all other data	https://www.singstat.gov.sg/-/media/files/news/press20022020.pdf
	CIA (Saudi Arabia, 2013)	https://web.archive.org/web/20201227110002/https://www.cia.gov/library/publications/the-world-factbook/rankorder/2172rank.html
	United Nations Development Programme (Qatar, 2013)	http://hdr.undp.org/en/content/income-gini-coefficient
Population Density (logged)	World Bank (2018)	https://data.worldbank.org/indicator/EN.POP.DNST
Percent Migrants	United Nations Population Division (2019) International Migrants as a Share of the Total Population	https://www.un.org/en/development/desa/population/migration/data/estimates2/countryprofiles.asp

Government Efficiency	World Bank (2016) Averaged Responses to *Wastefulness of government spending *Burden of government regulation *Efficiency of legal framework in settling disputes *Efficiency of legal framework in challenging regs *Transparency of government policymaking	https://tcdata360.worldbank.org/indicators/h8125e315?country=BRA&indicator=40979&viz=line_chart&years=2016
Tightness	Eriksson et al. (2021), updated from Gelfand et al. (2011)	https://osf.io/47pe8/ (data) https://osf.io/qg6xy/ (preregistration)
Collectivism	Hofstede G. Culture's consequences: International differences in work-related values. Sage, 1984. Data downloaded in March 2020 from https://www.hofstede-insights.com/product/compare-countries/	
Power Distance		
Authoritarianism	Polity5 (Annual Time-Series, "AUTOC", 2018)	https://www.systemicpeace.org/inscrdata.html
Median Age	CIA Factbook (2018)	https://en.wikipedia.org/wiki/List_of_countries_by_median_age
Days Until Lockdown	Number of days since the first case that it took to have mandated Shelter-in-Place Orders. In the Oxford Tracker, this is a minimum score of "2" on variable C6: "Require not leaving the house with exceptions for daily exercise, grocery shopping, and 'essential' trips" Downloaded November 24, 2020	https://covidtracker.bsg.ox.ac.uk
Government Stringency	Average stringency of government response from the Oxford Tracker from the earliest date available until October 15 (codebook: https://github.com/OxCGRT/covid-policy-tracker/blob/master/documentation/index_methodology.md The Oxford Government Stringency measure is an average of the following variables: C1 – closings of schools and universities C2 – closings of workplaces C3 – cancelling public events C4 – limits on private gatherings C5 – closing of public transport C6 – orders to "shelter-in-place" and otherwise confine to the home C7 – restrictions on internal movement between cities/regions C8 – restrictions on international travel (for foreign travelers) H1 – presence of public info campaigns Downloaded November 24, 2020	https://covidtracker.bsg.ox.ac.uk

Mortality Rate	World Bank (2018)	https://data.worldbank.org/indicator/SP.DYN.CDRT.IN
Relational Mobility	Thomson et al. (2018)	http://relationalmobility.org/#rmob-country-scores
Cold Stress	Van de Vliert et al., 2019. Dataset: The Global Ecology of Differentiation Between "Us" and "Them"	https://dataverse.nl/dataset.xhtml?persistentId=hdl:10411/YXI7WH
Heat Stress		
Rain Stress		
BCG Status	Berg et al. (2020).	https://advances.sciencemag.org/content/advances/suppl/2020/07/30/sciadv.abc1463.DC1/abc1463_SM.pdf
Population Size (logged)	United Nations Population Division (2020)	https://population.un.org/wpp/Download/Files/1_Indicators%20(Standard)/EXCEL_FILES/1_Population/WPP2019_POP_F01_1_TOTAL_POPULATION_BOTH_SEXES.xlsx
Number of SARs Cases	World Health Organization (November 1, 2002 to July 31, 2003) Data downloaded October 23, 2020 from Wikipedia	https://en.wikipedia.org/wiki/Severe_acute_respiratory_syndrome
Fear of Catching COVID-19	YouGov (2020) % fear score over the first 100 days after the country had its 1st COVID-19 case and the % fear score for the entire period from February 21st to September 24th. Data downloaded September 29, 2020	https://yougov.co.uk/topics/international/articles-reports/2020/03/17/fear-catching-covid-19

Appendix S2. Sample and Key Values.

Country	Cultural Tightness	Cases per Million	Deaths per Million	Test-Case Ratio
Algeria	0.69	1226.36	41.87	NA
Argentina	-0.53	20998.64	560.72	2.09
Armenia	0.21	20246.46	352.99	NA
Australia	-0.05	1073.03	35.45	297.97
Austria	0.21	6746.76	99.26	30.96
Bosnia and Herzegovina	-0.43	9821.95	296.27	NA
Botswana	0.86	2229.1	8.51	NA
Brazil	-0.38	24319.72	717.26	1.24
Canada	-0.14	5080.05	256.98	43.83
Chile	-0.34	25449.4	702.75	7.77
China	0.19	63.16	3.29	1760.08
Colombia	-0.58	18414.48	559.27	3.91
Czech Republic	-0.46	13914.49	114.86	11.36
Ecuador	-0.18	8522.33	697.5	2.71
Estonia	-0.47	3000.29	51.26	60.33
Finland	-0.28	2345.18	63.17	97.26
Germany	0.13	4160.19	116.18	55.3
Ghana	1.24	1518.14	9.98	10.66
Greece	-0.28	2297.5	46.24	62.19
Hungary	-0.60	4453.77	112.32	20.25
Iceland	0.04	11243.96	29.3	41.4
India	0.73	5340.9	81.28	12.38
Indonesia	0.50	1276.53	44.85	7.02
Iran	0.38	6165.22	352.47	8.55
Ireland	-0.18	9402.78	372.23	29.86
Israel	-0.40	34683.1	245.74	13.84
Italy	-0.06	6311.45	601.57	20.72
Ivory Coast	0.27	767.94	4.59	8.67
Japan	0.19	722.91	13.05	29.81
Kazakhstan	0.17	7709.61	114.18	21.94
Kenya	0.53	802.34	14.97	13.81
Latvia	-0.04	1620.19	21.74	125.31
Malaysia	0.22	560.13	5.25	98.56
Mexico	-0.35	6475.55	661.47	2.03
Mozambique	0.53	337.13	2.34	15.12
Netherlands	-0.54	11888.74	390.02	14.1
Nigeria	0.54	295.11	5.41	9.29
Peru	-0.34	26074.97	1018.35	0.73
Poland	-0.32	3960.8	87.41	24.15
Portugal	0.10	9149.42	208.69	31.15
Qatar	0.85	44706.81	77.06	6.64
Russia	-0.47	9279.26	160.97	38.98
Saudi Arabia	0.62	9796.73	147.27	21.15
Singapore	0.36	9895.49	4.79	56.83
Slovakia	-0.36	4437.1	13.01	24.53
South Korea	0.19	488.31	8.6	97.55
Spain	-0.30	19706.52	717.64	11.87
Sri Lanka	0.65	244.9	0.61	69.77
Sweden	0.34	10140.04	585.19	NA
Thailand	0.25	52.56	0.85	126.46
Trinidad and Tobago	-0.20	3711.35	66.45	NA
Turkey	0.29	4056.76	107.66	35.3
UAE	0.48	11267.19	45.7	101.68
Ukraine	-0.44	6430.71	121.23	9.71
United Kingdom	-0.21	9922.84	637.73	36.34
United States	-0.13	24108.22	657.7	16.28
Vietnam	0.39	11.55	0.36	1121.71

Note: The cultural tightness values in the table are from Eriksson et al. (2021) and were standardized in the regression analyses.

Supplemental References

1 Gelfand MJ, Raver JL, Nishii L, *et al.* Differences between tight and loose cultures: A 33-nation study. *Science* 2011; **332**: 1100–4.

2 Chua RYJ, Roth Y, Lemoine J-F. The impact of culture on creativity: How cultural tightness and cultural distance affect global innovation crowdsourcing work. *Adm Sci Q* 2015; **60**: 189–227.

3 Crossland C, Hambrick DC. Differences in managerial discretion across countries: how nation-level institutions affect the degree to which CEOs matter. *Strateg Manag J* 2011; **32**: 797–819.

4 Eun CS, Wang L, Xiao SC. Culture and R2. *J Financ Econ* 2015; **115**: 283–303.

5 Aktas M, Gelfand MJ, Hanges PJ. Cultural tightness–looseness and perceptions of effective leadership. *J Cross-Cult Psychol* 2016; **47**: 294–309.

6 Geeraert N, Li R, Ward C, Gelfand M, Demes KA. A tight spot: How personality moderates the impact of social norms on sojourner adaptation. *Psychol Sci* 2019; **30**: 333–42.

7 Jackson JC, van Egmond M, Choi VK, *et al.* Ecological and cultural factors underlying the global distribution of prejudice. *PLOS ONE* 2019; **14**: e0221953.

8 Taras V, Kirkman BL, Steel P. Examining the impact of Culture's consequences: A three-decade, multilevel, meta-analytic review of Hofstede's cultural value dimensions. *J Appl Psychol* 2010; **95**: 405–39.

9 Eriksson K, Strimling P, Gelfand MJ, Van Lange PAM *et al*. Perceptions of the appropriate response to norm violation in 57 Societies. Manuscript in press. *Nat Commun* 2021.

10 Roos P, Gelfand M, Nau D, Lun J. Societal threat and cultural variation in the strength of social norms: An evolutionary basis. *Organ Behav Hum Decis Process* 2015; **129**: 14–23.

11 Smaldino PE, Schank JC, McElreath R. Increased costs of cooperation help cooperators in the long run. *Am Nat* 2013; **181**: 451–63.

12 Hilbe C, Nowak MA, Sigmund K. Evolution of extortion in Iterated Prisoner's Dilemma games. *Proc Natl Acad Sci* 2013; **110**: 6913–8.

13 Huber PJ. The behavior of maximum likelihood estimates under nonstandard conditions. *Berkeley Symp Math Stat Probab* 1967; **1**: 221.

14 Rogers W. Regression standard errors in clustered samples. *Stata Tech Bull* 1994; **3**. https://econpapers.repec.org/article/tsjstbull/y_3a1994_3av_3a3_3ai_3a13_3asg17.htm (accessed Oct 22, 2020).

15 Salvador C, Berg M, Yu Q, Alvaro SM, Kitayama S. Relational mobility predicts the increased speed of the spread of COVID-19: A 37 country study. *Psych Sci* 2020; **31**: 1236-1244.

16 Thomson R, Yuki M, Talhelm T, *et al.* Relational mobility predicts social behaviors in 39 countries and is tied to historical farming and threat. *Proc Natl Acad Sci* 2018; **115**: 7521–6.

17 Berg MK, Yu Q, Salvador CE, Melani I, Kitayama S. Mandated Bacillus Calmette-Guérin (BCG) vaccination predicts flattened curves for the spread of COVID-19. *Sci Adv* 2020; **6**. DOI:10.1126/sciadv.abc1463.

18 Cao C, Li N, Liu L. Do national cultures matter in the containment of COVID-19? *Int J Sociol Soc Policy* 2020. DOI:10.1108/IJSSP-07-2020-0334.

19 Paul SR, Fung KY. A generalized extreme studentized residual multiple-outlier-detection procedure in linear regression. *Technometrics* 1991; **33**: 339–48.

20 Mu Y, Han, S, Gelfand, MJ. The role of gamma interbrain synchrony in social coordination when humans face territorial threats. *Soc Cogn Affect Neuro*, 2017; **12**: 1614-1623. DOI:10.1093/scan/nsx093